Multiparametric Study of an Eruptive Phase Comprising Unrest, Major explosions, Crater Failure, Pyroclastic Density Currents and Lava Flows: Stromboli volcano, 1 December 2020 – 30 June 2021

Supplementary Material (SM) - Materials and Methods

S. Calvari [1], F. Di Traglia [2], G. Ganci [1], V. Bruno [1], F. Ciancitto [1], B. Di Lieto [3], S. Gambino [1], A. Garcia [4], F. Giudicepietro [3], S. Inguaggiato [5], F. Vita [5], M. Cangemi [6], C. Inguaggiato [4,7], G. Macedonio [3], M. Mattia [1], L. Miraglia [1], T. Nolesini [8], M. Pompilio [9], P. Romano [3], G. Salerno [1], N. Casagli [2,10], G. Re[9], P. Del Carlo [9], A. Di Roberto [9], A. Cappello [1], C. Corradino [1], E. Amato [1,11], F. Torrisi [1,12], C. Del Negro[1], A.M. Esposito [3], W. De Cesare [3], T. Caputo [3] , M.F. Buongiorno [13], M. Musacchio [13], V. Romaniello [13], M. Silvestri [13], E. Marotta [3], R. Avino [3], G. Avvisati [3], P. Belviso [3]

[1] Istituto Nazionale di Geofisica e Vulcanologia, Osservatorio Etneo – Sezione di Catania, Piazza Roma 2, 95125 Catania, Italy.

[2] National Institute of Oceanography and Applied Geophysics—OGS, Borgo Grotta Gigante 42/C, 34010 Sgonico, Italy.

[3] Istituto Nazionale di Geofisica e Vulcanologia, Osservatorio Vesuviano, Via Diocleziano 328, 80124 Napoli, Italy.

[4] Istituto Nazionale di Geofisica e Vulcanologia, Sezione di Bologna. Via Donato Creti 12, 40128 Bologna, Italy.

[5] Istituto Nazionale di Geofisica e Vulcanologia, Sezione di Palermo, Via Ugo La Malfa 153, 90146 Palermo, Italy.

[6] DiSTeM, Università degli Studi di Palermo, via Archirafi 36, 90123 Palermo, Italy.

[7] Departamento de Geología, Centro de Investigación Científica y de Educación Superior de Ensenada, Baja California (CICESE), Carretera Ensenada-Tijuana 3918, Ensenada, Baja California, México.

[8] Università degli Studi di Firenze—Centro per la Protezione Civile, Piazza San Marco 4, 50121 Firenze, Italy.

[9] Istituto Nazionale di Geofisica e Vulcanologia, Sezione di Pisa, Via Cesare Battisti 53,

56125, Pisa, Italy.

[10] Dipartimento di Scienze della Terra, Università degli Studi di Firenze, Via La Pira 4, 50121 Firenze, Italy.

[11] Department of Mathematics and Computer Science, University of Palermo, Via Archirafi, 34, 90123 Palermo, Italy.

[12] Department of Electrical, Electronic and Computer Engineering, University of Catania, Viale Andrea Doria, 6, 95125 Catania, Italy.

[13] Istituto Nazionale di Geofisica e Vulcanologia, Osservatorio Nazionale Terremoti, Via di Vigna Murata 605, 00143 Rome, Italy.

SM.1 Monitoring cameras network and drone survey

The Istituto Nazionale di Geofisica e Vulcanologia (INGV) installed a network of thermal and visible cameras for volcanic monitoring purposes on the island of Stromboli more than 20 years ago (Bertagnini et al., 1999; Calvari et al., 2005; Zanon et al., 2009). The network now comprises 5 cameras allowing a view from different directions and perspectives, whose features are listed in Table SM1. The position of all permanent monitoring devices used in this paper is shown in Figure SM1.

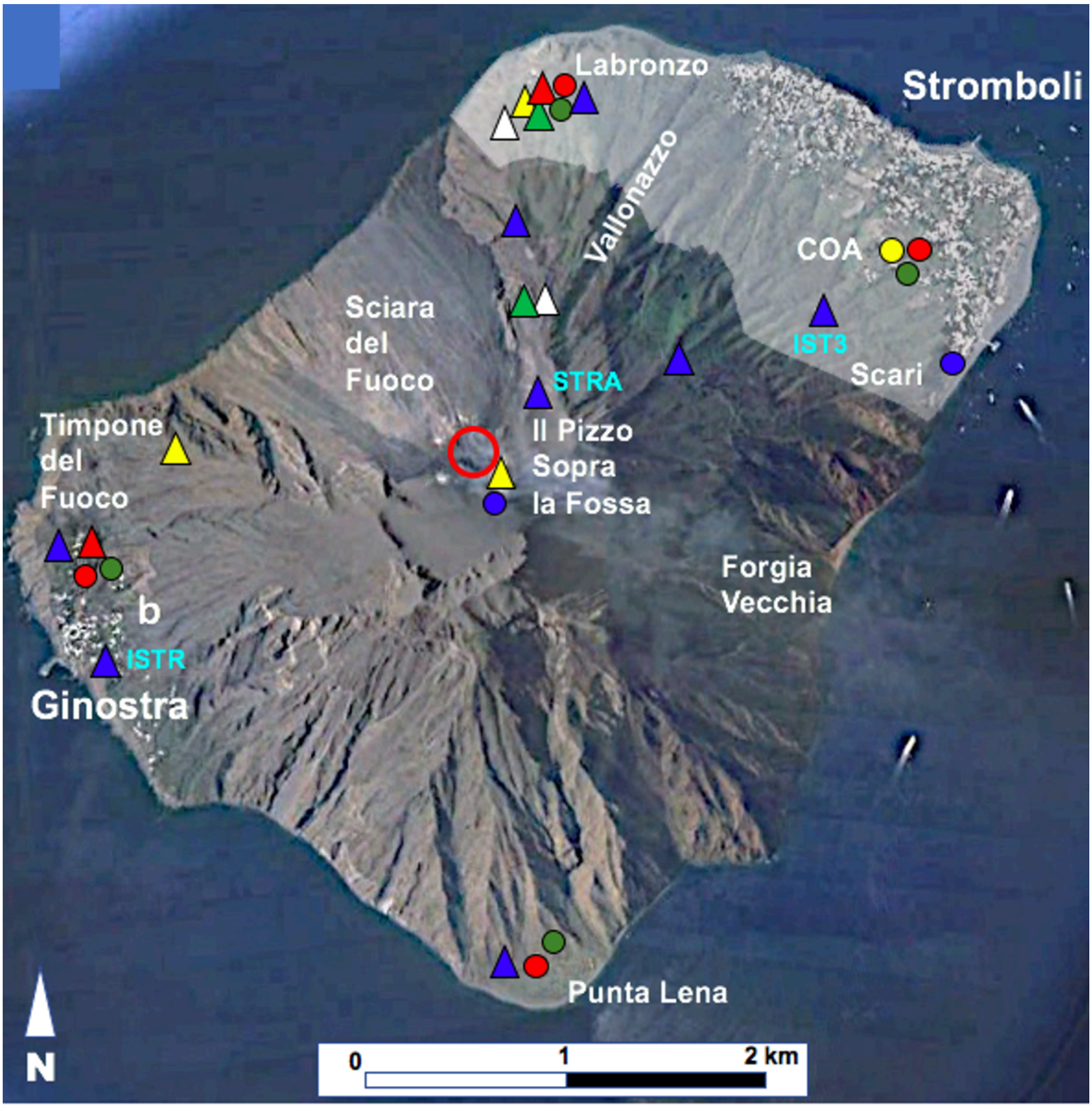

Figure SM1 - GoogleEarth satellite imagery (7 July 2019) of Stromboli island with the summit craters shown by the red empty circle, and indicating the distribution of the monitoring instruments used in this paper: yellow triangles: thermal cameras; white triangles: visible cameras; green triangles: GBInSARs; red triangles: tiltmeters; yellow circle: strainmeter; blue triangles: seismic stations; red circles: GNSS stations; green circles: FLAME stations for SO_2 measurements; blue circles: soil CO_2 monitoring stations. The light shaded area in the NE side of the island identifies the deposit of 19 May 2021 ash cloud.

To quantify the intensity and magnitude of the eruptive activity, we used software based on the images from the SPT thermal camera, the only one allowing an entire view of the whole crater terrace with the same visibility during day and night. The software uses a color threshold and takes into account saturated images, with the saturation area being set at > 100°C (Mattia et al., 2021). A tool analyzed the videos recorded by the camera (whose main features are listed in

Table SM1) and automatically detected the explosions from the summit craters, distinguishing two crater zones: a NE crater zone (NEC), and a SW crater zone (SWC) comprising the vents from the central crater zone (CC) and from the SW crater zone (Figure SM2).

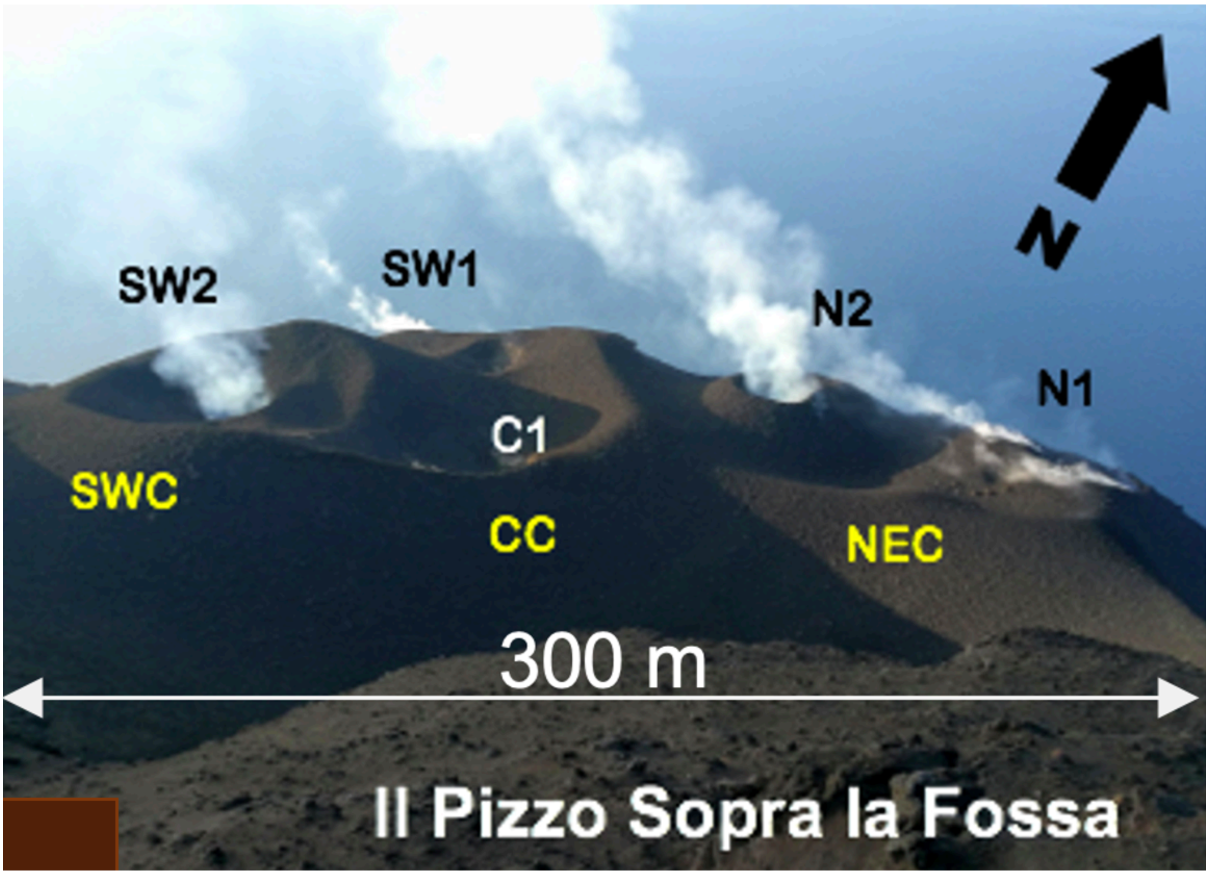

Figure SM2 - Photo of Stromboli taken by Francesco Ciancitto on 13 January 2020 from Il Pizzo Sopra la Fossa, showing from the South the whole crater terrace (the field of view is ~ 300 m wide), the summit crater zones (SWC = SW crater zone; CC = central crater zone; NEC = NE crater zone) and the active vents C1, N1, N2, SW1 and SW2.

For each explosive event the software records: (1) timing (hh:mm:ss in UTC), (2) duration (in seconds), (3) crater producing the event (either NEC or SWC+CC), (4) dispersion (area of the saturated thermal anomaly, expressed in pixels), and (5) indication of a grade of reliability of the detection (that is affected by weather conditions and integrity of the video files). In addition to the images from the camera network, for the reconstruction of the eruptive events we have also used photos taken during two helicopter surveys carried out on 19 May 2021 and 19 August 2021. Due to the flight path, these photos were taken at variable distances from the ground surface and from different viewing angles. We have estimated a distance from the surface between 500 m and 1000 m.

Table SM1. List of the monitoring cameras used in this paper and of their main features. SdF = Sciara del Fuoco. The field of view is considered at the crater rim.

Label	Camera Type	Location	Field of View (m)
SPT	Thermal FLIR A310	Pizzo Sopra La Fossa, 890 m a.s.l.	500 × 370
SPCT	Thermal FLIR A320	Punta dei Corvi, West SdF flank 85 m a.s.l.	2,150 × 1,613
SCT	Thermal FLIR A655sc	Labronzo, East SdF flank 165 m a.s.l.	807 × 605
SQV	Visible Sony FCB-EX480CP	East SdF flank, 390 m a.s.l.	657 × 493
SCV	Visible Mobotix M26	Labronzo, East SdF flank 163 m a.s.l.	1,776 × 1,274

A thermal overflight of the crater area of Stromboli was carried out on 21 September 2021 using a UAV (Unmanned Aerial Vehicle) SR-X4 quadcopter (MTOW-maximum take-off weight of 7 kg). This UAV has a robust radio connection, a flight autonomy of about 48 minutes and is equipped with a high resolution (640 × 512 pixel) and precision (± 5 °C) FLIR VUEPRO thermal imaging camera. We carried out a scheduled flight with a take-off point far from the craters (at the shelters located at 780 m a.s.l.). The surveys were done in conjunction with a thermal satellite passage, in conditions of non-solar radiation in the evening, with flight missions at a constant altitude of 120 m above the ground, obtaining more than 200 infrared (IR) images at a resolution of about 25 cm^2. The images were analyzed and post-processed with two dedicated softwares (Pix4d and Analyst). On the basis of the high-resolution point cloud topographic model, we obtained the plano-altimetric trend of the crater area. In order to evaluate morphological differences with a drone survey obtained in June 2020 (Civico et al., 2021), the two morphological profiles were superimposed.

SM.2 Seismic stations

In the period examined in this article, the Stromboli seismic network (Table SM2) was managed by the Osservatorio Vesuviano (INGV-OV) in Naples and by the Osservatorio Etneo (INGV-OE) in Catania, and comprised eight stations. In particular, six stations were equipped with CMG 40T Guralp broadband velocimeters (60 s - 50 Hz) and GAIA2 or GILDA digitizers produced by INGV (Orazi et al., 2006). Two other stations were equipped with very broadband (120 s) sensors and commercial digitizers (Table SM2). The seismic stations are distributed at different altitudes on the volcano, with the exception of the Sciara del Fuoco flank, which is inaccessible. Seismic data are transmitted to Stromboli data center or to the INGV Observatory in Lipari through a Wi-Fi network infrastructure or point-to-point links based on UHF digital radio-modems. Thus, the data produced by the seismic network are acquired and stored at the

Stromboli data center and at the Lipari INGV Observatory, then they are sent to the acquisition centers of INGV-OV and INGV-OE.

Table SM2. List of the seismic stations used in this paper and of their main features.

Label	Seismic station Type	Location	Seismic station transmission
STR1	BroadBand 60 s -50 Hz, 50 sps	Liscione	UHF COA
STR4	BroadBand 60 s -50 Hz, 50 sps	Punta Lena	UHF Lipari
STRA	BroadBand 60 s -50 Hz, 50 sps	Il Pizzo Sopra la Fossa	UHF COA
STRC	BroadBand 60 s -50 Hz, 50 sps	Ginostra Timpone del Fuoco	WiFi
STRE	BroadBand 60 s -50 Hz, 50 sps	Bastimento 450 m	UHF - Wi-Fi
STRG	BroadBand 60 s -50 Hz, 50 sps	Labronzo	WiFi
IST3	Very Broad Band 120 s -175 Hz, 100 sps	Osservatorio Fiorentini	UHF COA
ISTR	Very Broad Band 120 s -175 Hz, 100 sps	Ginostra	UHF Lipari

SM.3 GBInSAR

Interferometric Synthetic Aperture Radar (InSAR) is a remote sensing technique allowing detection and measurement of ground deformation of the target with centimeter to millimeter accuracy along the Line-Of-Sight (LOS), by means of the phase difference (interferogram) between two SAR images acquired over the same area at different epochs (temporal baseline) and with different sensor positions (spatial baseline), and provides an estimate of the ground displacement projected along the satellite LOS (Gabriel et al., 1989). In this work, InSAR technology was exploited through the use of two ground-based devices (GBInSAR) that emit and receive a burst of microwave pulses, repeating this operation while the sensor is moving, measuring the amplitude and the phase of the received radar signal (Rudolf et al., 1999; Antonello et al., 2004). The two GBInSAR devices are located in a stable area north of the SdF (Figure SM1), and are used to monitor the NE portion of the summit crater terrace and the northern portion of the SdF (Schaefer et al., 2019). In the Stromboli GBInSAR, the SAR technology is made possible by moving the real antennas along a rail (track), and the length of this rail (4 m long) determines the cross-range resolution of the acquired images (Antonello et al., 2004; Di Traglia et al., 2015). The ground LOS displacements are obtained from the interferograms, which in turn originate from phase information of “averaged” images, in that they are created by averaging every half hour the phase information derived from the various acquisitions (Di Traglia et al., 2015, 2021; Table SM3). A resample operation returns an image with the pixel size of about 2 m × 2 m along both range and cross range (Casagli et al., 2009). Pixel by pixel displacements staking algorithm allows the measurement of the cumulative displacements, whereas the time series of selected points (averaged over 5 × 5 pixels) are obtained from cumulative displacement maps with a precision in the displacement measurement of 0.5 mm (Antonello et al., 2004; Di Traglia et al., 2015, 2021). The features of the two GBInSAR devices are reported in Table SM3.

Table SM3. List of the monitoring GB-InSAR instruments used in this paper and their main features.

System	Revisiting time	Averaging interval	Look Angle / Heading Angle
GB-InSAR NE400	6 minutes	33 minutes	from 63.8° to 90.0° / from 143° to 217°
GB-InSAR NE190	7 minutes	30 minutes	from 65.0° to 113.5° / from 115° to 245°

SM.4 GNSS network

The GNSS (Global Navigation Satellite Systems) monitoring of ground deformations at Stromboli volcano started in June 1997, when the stations SPLN (Punta Lena), SPLB (Punta Labronzo) and STDF (Timpone del Fuoco) were installed at the base of the volcano, along the coastline (see Figure SM1 for stations location). The current configuration of the network includes a fourth station, SVIN (San Vincenzo or COA, Figure SM1) that was installed in 2003 and completes the geometry around the volcanic edifice. The GNSS data are processed on a daily basis by using a GAMIT/GLOBK software (Herring et al., 2015; 2018).

SM.5 Tiltmeters

At Stromboli, three bore-hole tiltmeters, 3 meters deep, were installed in 1992 at Punta Labronzo (PLB), Timpone Del Fuoco (TDF) and Punta Lena (PLN; Figure SM1) (Gambino et al., 2014). Moreover, between 2008 and 2010, two deep stations (-27 m from the ground surface) were installed at TDF and San Vincenzo Observatory (SVO), by using AGI Lily tiltmeters. At present, the PLB and TDF deep stations are active (red triangles in Figure SM1); their data are transmitted, in real-time, to INGV-OE.

SM.6 Strainmeters

In 2006 two Sacks-Evertson borehole dilatometers (Sacks et al., 1971; Roeloffs & Linde, 2007) were added to the Stromboli INGV geophysical network, with the support of the Italian Civil

Protection Department, of the Università degli Studi di Salerno (Italy) and of the Carnegie Institution of Washington DC (USA). The Sacks-Evertson borehole dilatometers are a special kind of strainmeter, capable of recording volumetric strain changes with a nominal resolution up 10^{-12} in strain, depending on the final response of the coupling of the instruments with the surrounding rock. Currently, the SVO instrument (Figure SM1), situated in the village of Stromboli, about 2.5 km northeast from the summit craters, is the only functioning strainmeter at Stromboli volcano. The device was installed at a depth of 120 m from the ground surface in massive rock, providing a reliable signal with a sensitivity of 1×10^{-11} per digital count (Di Lieto et al., 2020).

SM.7 Geochemical stations

SM.7.1 SO_2 flux from the summit craters

The bulk SO_2 flux released by the summit craters of the volcano is measured during daylight hours by the FLAME (FLux Automatic MEasurement) ultraviolet DOAS scanning spectrometer network (e.g. Salerno et al., 2009a). The network consists of four ultraviolet scanning spectrometers placed near the coast of the island and intercepting the plume from a distance of ~2 km from the summit craters of Stromboli. Each instrument scans the sky over 156° from horizon to horizon every 5 min during daylight. Open-path ultraviolet spectra are reduced on-site applying the differential optical absorption spectroscopy method (e.g. Platt and Stutz 2008) and using a modeled clear sky spectrum (Salerno et al. 2009b; Campion et al. 2015; Merucci et al. 2011). SO_2 mass emission rates are automatically computed by inverting the SO_2 volcanic column amounts plume-profiles; uncertainty in SO_2 flux ranges between -22 and +36% (Salerno et al. 2009a; Salerno et al. 2018). Details and configuration of the network are given in Burton et al. (2009), and the sites of the FLAME stations are shown in Figure SM1.

SM.7.2 CO_2 flux from the ground

Volatile degassing at Stromboli occurs through volcanic plumes, soil degassing and thermal aquifers. Its monitoring represents a useful tool for investigating the volcanic plumbing system and tracking the changes in volcanic activity, with particular reference to paroxysms and lava flows. Soil CO_2 flux from the summit and peripheral areas has been monitored during the last 20 years by a geochemical network (Inguaggiato et al., 2011, 2017, 2018) consisting of two stations, located in the Scari area (STR01) and at Il Pizzo Sopra La Fossa (STR02; Figure SM1). These stations utilize the accumulation chamber method and are equipped with infrared sensors to measure the CO_2 concentration; additional environmental sensors measure air temperature and relative humidity, atmospheric pressure and wind speed and direction. The stations are powered by batteries recharged by solar panels.

SM.8 Satellites

MODIS satellite data are routinely processed via the HOTSAT satellite thermal system at Stromboli volcano (Ganci et al., 2011; 2016). MODIS data, acquired at spatial resolution of 1 km at nadir, allow distinguishing not only the effusive phases, but also the intense spattering activity at the summit craters. The Sea and Land Surface Temperature Radiometer (SLSTR), on board the polar Sentinel-3A and Sentinel-3B satellites, are used to generate a Level-2 product (SL_2_FRP) related to actively burning fires and this product is available in the web portal of EU Copernicus Programme (https://scihub.copernicus.eu/). The VIIRS Level-2 active fire products are distributed by the LANCE/FIRMS platform (https://firms.modaps.eosdis.nasa.gov/). VIIRS and SLSTR-SENTINEL 3 sensors are used to monitor volcanic thermal anomalies in the FLOWSAT platform. VIIRS sensor provides an improved spatial resolution, namely 375 m and 725 m, thus allowing a finer thermal anomalies detection and SLSTR sensor has dedicated fires channels with higher saturation temperature.

Changes in Land Surface Temperature (LST) can be monitored with MODIS LST data providing two night-time temperature measurements per day with 1-km spatial resolution and an inversion accuracy of approximately 1 K (Wan, 2014). We only use nighttime LST data for the analysis due to the absence of solar heating, leading to measurements that are predominantly gathered from surface and underground thermal sources. Changes in LST can be related to different volcanic sources, such as lava flow emission, explosions and both pre- and post-eruptive gas emissions (Marotta et al., 2015; Corradino et al., 2021a). We use the general anomaly method (Wu et al., 2016) to monitor changes in temperature due to volcanic processes.

To date, optical satellite sensors acquiring in the TIR range and having the best spatial resolution (70–100 m) are the Advanced Spaceborne Thermal Emission and Reflection Radiometer (ASTER, Yamaguchi et al., 1998), TIRS on Landsat 8 (L8, Roy et al., 2014) and the last ECOsystem Spaceborne Thermal Radiometer Experiment on Space Station (ECOSTRESS, Fisher et al., 2015) on board the International Space Station. These sensors allow detecting thermal anomalies and hot spots in small areas (in the order of hundreds of meters) and offer the possibility to estimate the land surface temperature (LST), highlighting the main surface thermal changes, potentially related to underground energy sources (Silvestri et al., 2020a). Specifically, data acquired by ASTER, L8 and ECOSTRESS have been rescaled to 90 m to standardize the intercomparison (Silvestri et al., 2020b).

Sentinel-1 SAR images are made available at level-1C Ground Range Detected (GRD) in Google Earth Engine (GEE) platform, where they are already preprocessed based on the algorithms implemented by the Sentinel-1 Toolbox software (Karamanolakis, et al., 2019).

SM.9 Erupted products

On 19 May 2021, a few hours after the NEC collapse, samples of ash were collected following a SE-NW traverse across the Stromboli village, downwind from the crater area at variable elevation from 0 to 150 m a.s.l. The ash was collected on clean flat surfaces and the sampling area was measured. Sample weight of materials was measured in the lab after drying. For comparison we also investigated fresh-lapilli sampled on Il Pizzo Sopra la Fossa area on 16 May, that represent the magma feeding the persistent summit activity three days before the 19 May 2021 event.

External surface and morphologies of clasts were observed using a scanning electron microscope (SEM) Zeiss EVO MA at the INGV-Sezione di Pisa (INGV-Pisa). Bulk tephra were epoxy mounted for further componentry, textural and geochemical investigations. We carried out grain size distributions (GSD) with image analysis techniques, on a mosaic of pictures (resolution of 2048 × 1536 pixel) acquired for each sample at magnification of 200 ×, by the use of the ImageJ software. The GSD lower limit was set at 5φ, that corresponds to particles with diameter > 32 μm. Geochemical analyses were performed on apparently fresh glassy clasts at INGV-Pisa and INGV-OE using Aztec Oxford energy dispersive X-ray detector (accelerating voltage 20 kV, beam current 1 nA, working distance 8.5 mm) on raster mode (10 micron). The VG-2 basaltic glass secondary standard was analyzed repeatedly during the EDS acquisitions and in both laboratories to test the accuracy of the results.

References

Antonello G., Casagli N., Farina P., Leva D., Nico G., Sieber A. J., & Tarchi D. (2004). Ground-based SAR interferometry for monitoring mass movements. Landslides, 1(1), 21-28.

Bertagnini A., Coltelli M., Landi P., Pompilio M., Rosi M. (1999). Violent explosions yield new insights into dynamics of Stromboli Volcano. EOS Transactions, AGU, 80, 52, 633-636.

Burton, M. R., Caltabiano, T., Murè, F., Salerno, G., and Randazzo, D. (2009). SO_2 flux from Stromboli during the 2007 eruption: results from the FLAME network and traverse measurements. J. Volcanol. Geotherm. Res. 182, 214–220. doi:10.1016/j.jvolgeores.2008.11.025

Calvari, S., Spampinato, L., Lodato, L., Harris, A.J.L., Patrick, M.R., Dehn, J., Burton, M.R., Andronico, D. (2005). Chronology and complex volcanic processes during the 2002-2003 flank eruption at Stromboli volcano (Italy) reconstructed from direct observations and surveys with a hand-held thermal camera. J. Geophys. Res. 110, B02201, doi:10.1029/2004JB003129.

Campion, R., Delgado-Granados, H., and Mori, T. (2015). Image-based correction of the light dilution effect for SO2 camera measurements. J. Volcanol. Geotherm. Res. 300, 48–57. doi: 10.1016/j.jvolgeores.2015.01.004

Casagli, N., Tibaldi, A., Merri, A., Del Ventisette, C., Apuani, T., Guerri, L., Fortuny-Guasch, J., Tarchi, D. (2009). Deformation of Stromboli Volcano (Italy) during the 2007 eruption revealed by radar interferometry, numerical modelling and structural geological field data. Journal of Volcanology and Geothermal Research, 182(3-4), 182-200.

Civico, R.; Ricci, T.; Scarlato, P.; Andronico, D.; Cantarero, M.; Carr, B.B.; De Beni, E.; Del Bello, E.; Johnson, J.B.; Kueppers, U.; et al. (2021). Unoccupied Aircraft Systems (UASs) Reveal the Morphological Changes at Stromboli Volcano (Italy) before, between, and after the 3 July and 28 August 2019 Paroxysmal Eruptions Remote Sens. 2021, 13, 2870. https://doi.org/10.3390/rs13152870

Corradino C., Amato E., Torrisi F., Calvari S., Del Negro C. (2021a) - Classifying Major Explosions And Paroxysms At Stromboli Volcano (Italy) From Space. Remote Sensing, 2021, 13, 4080. https://doi.org/ 10.3390/rs13204080.

Di Lieto, B.; Romano, P.; Scarpa, R.; Linde, A. T. Strain signals before and during paroxysmal activity at Stromboli volcano, Italy. Geophys. Res. Lett., 2020, Vol. 47, https://doi.org/10.1029/2020GL088521.

Di Traglia, F., Battaglia, M., Nolesini, T., Lagomarsino, D., & Casagli, N. (2015). Shifts in the eruptive styles at Stromboli in 2010–2014 revealed by ground-based InSAR data. Scientific reports, 5, 13569.

Di Traglia, F., De Luca C., Manzo M., Nolesini, T., Casagli N., Lanari R., Casu F. (2021) - Joint exploitation of space-borne and ground-based multitemporal InSAR measurements for volcano monitoring: The Stromboli volcano case study. Remote Sens. of Environment 260, 112441, https://doi.org/10.1016/j.rse.2021.112441.

Fisher, J. B., Hook, S., Allen, R., Anderson, M. C., French, A. N., Hain, C., ... & Wood, E. F. (2015). ECOSTRESS: NASA's next-generation mission to measure evapotranspiration from the International Space Station. In AGU Fall Meeting Abstracts; AGU: Washington, DC, USA

Gabriel, A. K., R. M. Goldstein, and H. A. Zebker (1989), Mapping small elevation changes over large areas: Differential interferometry, J. Geophys. Res., 94, 9183–9191, doi:10.1029/JB094iB07p09183.

Gambino, S., Falzone, G., Ferro, A., & Laudani, G. (2014). Volcanic processes detected by tiltmeters: A review of experience on Sicilian volcanoes. Journal of Volcanology and Geothermal Research, 271, 43–54. https://doi.org/10.1016/j.jvolgeores.2013.11.007.

Ganci, G., Bilotta, G., Cappello, A., Hérault, A., Del Negro, C., 2016. HOTSAT: a multiplatform system for the satellite thermal monitoring of volcanic activity. Geological Society of London, Special Publications 426, 207–221. https://doi.org/10.1144/SP426.21.

Ganci, G., Vicari, A., Fortuna, L., Del Negro, C., 2011. The HOTSAT volcano monitoring system based on a combined use of SEVIRI and MODIS multispectral data. Ann. Geophys. 54, 5. https://doi.org/10.4401/ag-5338. 2011.

Herring, T.A., Floyd, M.A., King, R.W., McClusky, S.C. (2015). GLOBK: Global Kalman Filter VLBI and GPS Analysis Program, Reference Manual. Mass. Inst. of Technol., Cambridge.

Herring, T.A., King, R.W., Floyd, M.A., McClusky, S.C. (2018). GPS Analysis at MIT, GAMIT Reference Manual. Mass. Inst. of Technol., Cambridge.

Inguaggiato, S., Diliberto, I. S., Federico, C., Paonita, A., and Vita, F. (2018). Review of the evolution of geochemical monitoring, networks and methodologies applied to the volcanoes of the Aeolian Arc (Italy) *Earth-Science Reviews* 176, 241-276. https://doi.org/10.1016/j.earscirev.2017.09.006

Inguaggiato, S., Vita, F., Rouwet, D., Bobrowski, N., Morici, S., and Sollami, A. (2011). Geochemical evidence of the renewal of volcanic activity inferred from CO_2 soil and SO_2 plume fluxes: the 2007 Stromboli eruption (Italy). Bull. Volcanol. 73, 4, 443-456.

Inguaggiato, S., Vita, F., Cangemi, M., Mazot, A., Sollami, A., Calderone, L., Morici, S., and Jacome Paz, M.P. (2017). Stromboli volcanic activity variations inferred from observations of fluid geochemistry: 16 years of continuous monitoring of soil CO_2 fluxes (2000–2015). *Chemical Geology* https://doi.org/10.1016/j.chemgeo.2017.01.030

Inguaggiato, S., Vita, F., Cangemi, M., Calderone, L. (2019). Increasing Summit Degassing at the Stromboli Volcano and Relationships with Volcanic Activity (2016–2018). *Geosciences* 9, 176.

Karamanolakis, G., Hsu, D., Gravano, L. (2019). Weakly Supervised Attention Networks for Fine-Grained Opinion Mining and Public Health; Association for Computational Linguistics (ACL): Stroudsburg, PA, USA. pp. 1–10.

Marotta, E., Calvari, S., Cristaldi, A., D'Auria, L., Di Vito, M.A., Moretti, R., Peluso, R., Spampinato, L., and Boschi, E. (2015). Reactivation of Stromboli's summit craters at the end of the 2007 effusive eruption detected by thermal surveys and seismicity. *J. Geophys. Res. solid earth* 120, doi:10.1002/2015JB012288

Mattia, M., Di Lieto, B., Ganci, G.; Bruno, V.; Romano, P.; Ciancitto, F.; De Martino, P.; Gambino, S.; Aloisi, M.; Sciotto, M.; et al. (2021). The 2019 Eruptive Activity at Stromboli Volcano: A Multidisciplinary Approach to Reveal Hidden Features of the "Unexpected" July 3 Paroxysm. *Remote Sens*. 13, 4064. https:// doi.org/10.3390/rs13204064.

Merucci, L., Burton, M., Corradini, S., and Salerno, G.G., (2011). Reconstruction of SO_2 flux emission chronology from space-based measurements. *J. Volcanol. Geother. Res*. 206, 80–87.

Orazi, M., Martini, M., and Peluso, R. (2006). Data acquisition for volcano monitoring. *Eos Trans. Am. Geophys. Union* 87(38), 385-392.

Platt, A., and Stutz, U. (2008). Differential Optical Absorption Spectroscopy - Principles and Applications. Heidelberg: Springer, doi: 10.1007/978-3-540- 75776- 4

Roeloffs, E.A. and Linde, A.T. (2007). Borehole observations of continuous strain and fluid pressure. In: Volcano Deformation. Springer Praxis Books. Springer, Berlin, Heidelberg. https://doi.org/10.1007/978-3-540-49302-0_9

Roy, D. P., Wulder, M. A., Loveland, T. R., Woodcock, C. E., Allen, R. G., Anderson, M. C., ... and Scambos, T. A. (2014). Landsat-8: Science and product vision for terrestrial global change research. *Remote sensing Envir*. 145, 154-172.

Rudolf, H., Leva, D., Tarchi, D., and Sieber, A. J. (1999). A mobile and versatile SAR system. In: *IEEE 1999 International Geoscience and Remote Sensing Symposium. IGARSS'99* (Cat. No. 99CH36293) (Vol. 1, pp. 592-594). IEEE.

Sacks, S., Suyehiro, S., Evertson, D. W., and Yamagishi Y. (1971). Sacks-Evertson strainmeter, its installation in Japan and some preliminary results concerning strain steps. *Pap. Meteorol. Geophys*. 22, 195–208.

Salerno, G. G., Burton, M. R., Oppenheimer, C., Caltabiano, T., Randazzo, D., Bruno, N., et al. (2009a). Three-years of SO2 flux measurements of Mt. Etna using an automated UV scanner array: comparison with conventional traverses and uncertainties in flux retrieval. *J. Volcanol. Geotherm. Res*. 183, 76–83. doi: 10.1016/j.jvolgeores.2009.02.013

Salerno, G.G., Burton, M.R., Oppenheimer, C., Caltabiano, T., Tsanev, V., and Bruno, N. (2009b). Novel retrieval of volcanic SO2 abundance from ultraviolet spectra. *J. Volcanol. Geotherm. Res*. 181, 141–153. doi: 10.1016/j.jvolgeores. 2009.01.009.

Salerno, G.G., Burton, M., Di Grazia, G., Caltabiano, T., and Oppenheimer, C. (2018). Coupling Between Magmatic Degassing and Volcanic Tremor in Basaltic Volcanism. *Front. Earth Sci*. 6, 157. doi: 10.3389/feart.2018.00157.

Schaefer, L.N., Di Traglia, F., Chaussard, E., Lu, Z., Nolesini, T., and Casagli, N. (2019). Monitoring volcano slope instability with Synthetic Aperture Radar: A review and new data from Pacaya (Guatemala) and Stromboli (Italy) volcanoes. *Earth-Science Reviews* 192, 236-257.

Silvestri, M., Marotta, E., Buongiorno, M.F., Avvisati, G., Belviso, P., Bellucci Sessa, E., Caputo, T., Longo, V., De Leo, V. and Teggi, S., (2020a). Monitoring of Surface Temperature on Parco delle Biancane (Italian Geothermal Area) Using Optical Satellite Data, UAV and Field Campaigns. *Remote Sens.* 12(12), 2018. https://doi.org/10.3390/rs12122018

Silvestri, M., Romaniello, V., Hook, S., Musacchio, M., Teggi, S. and Buongiorno, M.F. (2020b). First Comparisons of Surface Temperature Estimations between ECOSTRESS, ASTER and Landsat 8 over Italian Volcanic and Geothermal Areas. *Remote Sens.* 12(1), 184. https://doi.org/10.3390/rs12010184

Wan, Z. (2014). New refinements and validation of the collection-6 MODIS land-surface temperature/emissivity product. *Remote Sens. Environ*. 140, 36–45.

Wu, L., Zheng, S., De Santis, A., Qin, K., Di Mauro, R., Liu, S., and Rainone, M.L. (2016). Geosphere coupling and hydrothermal anomalies before the 2009 Mw 6.3 L'Aquila earthquake in Italy. *Nat. Hazards Earth Syst. Sci*., 16, 18.

Yamaguchi, Y., Kahle, A.B., Tsu, H., Kawakami, T., and Pniel, M. (1998). Overview of advanced spaceborne thermal emission and reflection radiometer (ASTER). *IEEE Trans. geosc. remote sens.* 36(4), 1062-1071.

Zanon, V., Neri, M., and Pecora, E. (2009). Interpretation of data from the monitoring thermal camera of Stromboli volcano (Aeolian Islands, Italy). *Geol. Mag*. 146(4), 591-601.